

Microwave-accelerated metal-enhanced fluorescence: application to detection of genomic and exosporium anthrax DNA in <30 seconds

Kadir Aslan,^a Yongxia Zhang,^a Stephen Hibbs,^b Les Baillie,^{†b} Michael J. R. Previte^a and Chris D. Geddes^{*a}

Received 24th May 2007, Accepted 29th August 2007

First published as an Advance Article on the web 11th September 2007

DOI: 10.1039/b707876e

We describe the ultra-fast and sensitive detection of the gene encoding the protective antigen of *Bacillus anthracis* the causative agent of anthrax. Our approach employs a highly novel platform technology, Microwave-Accelerated Metal-Enhanced Fluorescence (MAMEF), which combines the use of Metal-Enhanced Fluorescence to enhance assay sensitivity and focused microwave heating to spatially and kinetically accelerate DNA hybridization. Genomic and exosporium target DNA of *Bacillus anthracis* spores was detected within a minute in the nanograms per microliter concentration range using low-power focused microwave heating. The MAMEF technology was able to distinguish between *B. anthracis* and *B. cereus*, a non-virulent close relative. We believe that this study has set the stage and indeed provides an opportunity for the ultra-fast and specific detection of *B. anthracis* spores with minimal pre-processing steps using a relatively simple but cost-effective technology that could minimize casualties in the event of another anthrax attack.

Introduction

The nature of bio-terrorism is such that an aggressor is likely to strike at a time and place calculated to induce maximum terror through mass casualties. In the absence of specific intelligence, real-time detection and diagnostic assays are essential tools in managing the consequences of an attack. Unfortunately, traditional laboratory-based assays can take several days to produce definitive results. In the context of a biological attack, this is an unacceptable delay if resulting casualties are to be minimized. The need for 'real-time' (<60 min) detection has led to the development of technologies based on DNA (PCR) and protein (antibody) targets¹ which, while relatively quick, suffer from the need for additional sample processing – to remove inhibitory compounds such as blood – and the amplification steps.² The ideal detector would be a device that is simple to use, hand-held, extremely rapid, and inexpensive, combines high specificity with sensitivity in the presence of organic material such as blood, and is also capable of detecting more than one agent.

The credentials of *Bacillus anthracis*, the causative agent of anthrax, as a bio-terror agent were confirmed by the 2001 postal attacks in the USA. The organism is able to infect *via* the aerosol route with a reported mortality rate in untreated individuals of >80%.^{3,4} Early treatment is essential as animal studies suggest that the disease reaches a point at which

antibiotics are no longer effective due to the accumulation of a lethal level of toxin.^{5,6} The bacterium produces a tripartite toxin consisting of two enzymatically active subunits – lethal factor (LF) and edema factor (EF) – which combine with the protective antigen (PA), the non-toxic cell-binding component, to form lethal toxin (LeTx) and edema toxin, respectively.⁷ Given the central role of this toxin in pathology, the ability to quickly detect the presence of PA or the gene encoding it in a biological sample would enable clinicians to institute timely treatment and thus minimize the number of casualties sustained in the event of a biological attack.

In this regard, one can find many new approaches to faster detection of *B. anthracis* using a variety of techniques including Surface-Enhanced Raman Spectroscopy,^{8,9} colorimetric detection based on specific aggregation gold nanoparticles,^{10,11} fluorescence polarization¹² and fluorescence resonance energy transfer (FRET) in the literature.¹³ However, all of these assays still require incubation times in excess of minutes. Recently, a new platform technology called Microwave-Accelerated Metal-Enhanced Fluorescence (MAMEF), that produces definitive results for the fluorescence-based bioassays within a *few seconds*, was introduced and demonstrated for the ultra-fast and sensitive detection of proteins^{14,15} and DNA hybridization assays.¹⁶ MAMEF technology couples the benefits of two technologies: (i) Metal-Enhanced Fluorescence (MEF) which increases the sensitivity of fluorescence-based bioassays,^{17–19} and (ii) low-power microwave heating which reduces the bioassay run time by kinetically accelerating the biological recognition events localized around the surface-bound nanostructures. The benefits of MEF can be visually demonstrated (Fig. 1a): a greater fluorescence emission is observed from fluorophores in close proximity to silver nanoparticles as compared to *unsilvered* glass. This phenomenon is due to the enhancement of fluorescence emission by the silver nanoparticles (that is,

^aInstitute of Fluorescence, Laboratory for Advanced Medical Plasmonics, Medical Biotechnology Center, University of Maryland Biotechnology Institute, 725 West Lombard St., Baltimore, MD 21201, USA. E-mail: geddes@umbi.umd.edu

^bBiodefense Initiative, Medical Biotechnology Center, University of Maryland Biotechnology Institute, 725 West Lombard St., Baltimore, MD 21201, USA

[†] Current address: Welsh School of Pharmacy, Cardiff University, Redwood Building, King Edward VII Avenue, Cardiff, Wales, UK CF10 3NB.

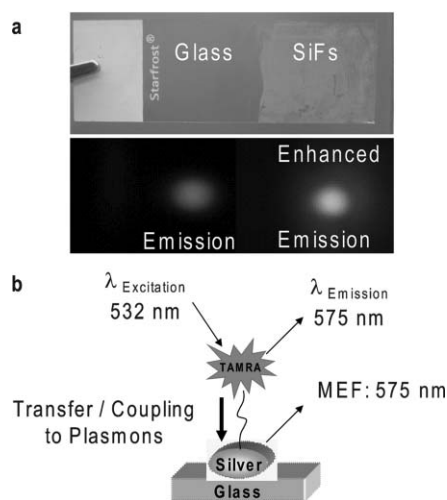


Fig. 1 (a) Photographs: silver island films (SiFs)-deposited glass substrate and real color emission of TAMRA on glass and SiFs taken through a 532 nm notch filter. (b) Current description of the metal-enhanced fluorescence (MEF) phenomenon whereby fluorescence emission from the fluorophores is partially plasmon coupled and the system (fluorophore and SiFs) radiates. TAMRA: tetramethylrhodamine.

MEF): the excited fluorophores partially transfer their energy to the silver nanoparticles where it is efficiently radiated and the emission from the fluorophore–silver ‘system’ becomes greater than the emission from fluorophores alone, *i.e.* amplified (Fig. 1b).²⁰ It is this unique combination of enhanced fluorescence emission and a *significantly* reduced bioassay run time that makes MAMEF a very powerful technology for fluorescence-based, ultra-fast and sensitive bioassays.¹⁴ A unified description of MEF has recently been postulated by Geddes and co-workers.²¹

In this paper, we present the ultra-fast and sensitive detection of target DNA encoding a region of the PA gene essential for biological activity, using the MAMEF platform technology. Employing this approach we are able to detect the presence of nanogram per microliter quantities of target DNA in a purified total genome extract within 30 s. We also determined the ability of the assay to detect target DNA on the surface of spores, the form of the organism most likely to be encountered during a biological attack. The feasibility of using PCR to detect DNA targets on the surface of unprocessed *B. anthracis* spores has been demonstrated with detection times of between 1 and 2 h and a sensitivity limit of 10² spores per reaction.^{22,23} Using MAMEF, we detected the presence of nanogram per microliter levels of target DNA in isolated spore surface extracts within 30 s. Moreover, the assay was able to distinguish between *B. anthracis* and *B. cereus*, a non-virulent, genetic close relative.

Experimental

Materials

Silver nitrate (99.9%), sodium hydroxide (99.996%), ammonium hydroxide (30%), D-glucose and premium quality

APS-coated glass slides (75 × 25 mm) were obtained from Sigma-Aldrich.

Bacterial strains: the Sterne, 34F2 strain of *Bacillus anthracis*, an attenuated variant employed extensively as an animal vaccine, a germination-deficient variant (Δ gerH) of *B. anthracis* Sterne 34F2²⁴ and the *B. cereus*-type strain ATCC 14579²⁵ were obtained from the Biological Defense Research Directorate, Naval Medical Research Center, Silver Spring, MD. Organisms were stored in 10% glycerol L broth at 20 °C. Difco L agar and Difco L broth were obtained from Becton Dickinson and Company (Becton Drive, Franklin Lakes, NJ) and made up as per the manufacturers’ instructions.

Methods

Design of anchor and fluorescent probes. Probes specific for a highly conserved region within the gene encoding PA were designed using the sequence published by Welkos *et al.*²⁶ (GenBank Accession No. M22589). The anchor and fluorophore-labeled probes were designed to bind to the negative strand (Fig. 2b). The region of homolog of the anchor probe comprised 17 nucleotides (nt) from 3943–3959 (Welkos’s numbering scheme). This region of homolog was preceded by a run of 10 consecutive Ts which were included to increase the flexibility of the probe when bound to the silver surface.²⁷ This was achieved by the inclusion of a C at the terminal of the probe to which a thiol group was added. The fluorophore-labeled probe consisted of a region of 22 nucleotides homologous to the sequence at positions 3970–3391. A TAMRATM NHS Ester Dye was attached to the first nucleotide which corresponded to position 3970. To aid assay development the target region was also synthesized. Probes and the target sequence were purchased from IDT (Coralville, IA).

Genomic DNA extraction. Bacteria of the Sterne 34F2 strain of *B. anthracis* were grown in Brain Heart Infusion (BHI) broth and genomic DNA extraction was carried out using a Wizard Genomic DNA extraction kit (Promega Corp, Madison, WI) following the manufacturer’s recommended procedures. The concentration and purity of the DNA were determined by absorbance measurements.

Production of anthrax spores. Spores of a germination-deficient variant (Δ gerH) of *B. anthracis* Sterne 34F2 and the *B. cereus*-type strain ATCC 14579 were prepared as previously described.²⁸ Briefly, a single colony harvested from an overnight culture grown on L agar at 37 °C were used to inoculate 100 mL of L broth in a 250 mL Duran bottle. The culture was incubated at 37 °C on an orbital shaker (200 rpm) for 6 h. At the end of this period, 3 mL of culture was transferred to a 225 mL vented tissue flask (Corning Inc) containing 12 mL isolation agar. The inoculation flasks were incubated at 30 °C until 99–100% of the organisms had formed endospores (microscopic examination/phase contrast). The percentage spore yield was determined by comparing colony counts of heated (70 °C for 20 min) and unheated samples. Endospores were harvested by adding 20 mL of sterile phosphate buffered saline (PBS) to the flask. The re-suspended endospores from 20

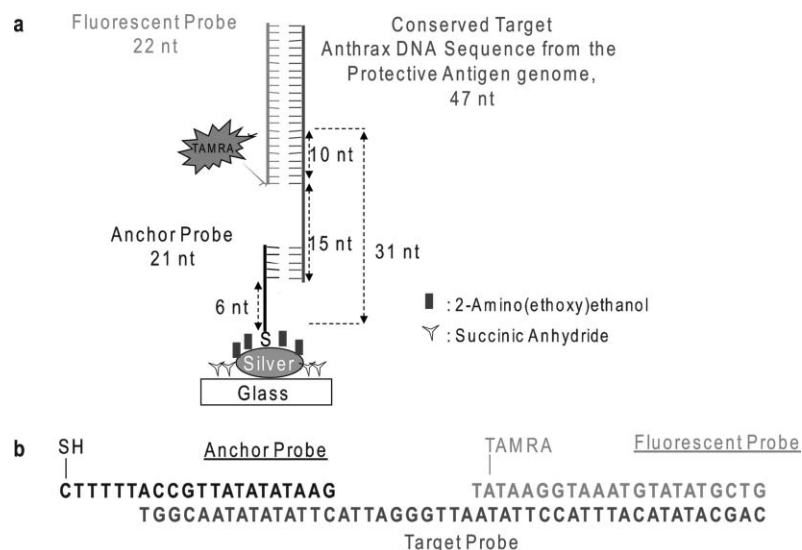


Fig. 2 (a) Experimental design depicting the organization of the DNA oligomers on silver island films (SiFs) used for the detection of *B. anthracis*. (b) Specific sequence of the DNA oligomers used. In order to minimize the non-specific adsorption of oligomers the glass and SiFs were treated with succinic anhydride and 2-amino(ethoxy)ethanol, respectively.

flasks were pooled and centrifuged at 4200 rpm for 10 min at 4 °C. The resulting pellet was re-suspended in 200 mL of sterile PBS and centrifuged. This process was repeated a further ten times to remove material loosely associated with the spore surface.

Isolation of exosporium. The exosporium was removed from the surface of washed spores by sonication.^{29,30} In this regard, first the spores were centrifuged at 10 000 g for 10 min at 4 °C. Pellets were re-suspended to approximately 3×10^7 spores mL⁻¹ in 50 mM Tris-HCl, 0.5 mM EDTA buffer (pH 7.5). All subsequent manipulations were at 4 °C. Spores were sonicated (Branson Sonifier 150; Branson Ultrasonics Co., Danbury, CT) with maximum power (amplitude, 12 μ m; 10 min/50 W) for seven one-minute bursts, each separated by 2 min of cooling on ice.²⁹ This causes partial fragmentation of the exosporium without disrupting the integrity of the spore.²⁹ Exosporium fragments were separated from spores by centrifugation at 9000 g for 15 min at 4 °C. The spore pellets were washed once in PBS, and the exosporium-containing supernatants were pooled and then centrifuged again to remove the remaining spores. Any residual endospores in the exosporium-containing supernatant were removed by filtration through 0.45 μ m and/or 0.2 μ m low-protein-binding filters (Acrodisc syringe filter; Pall Co., Timonium, MD).

Formation of silver island films (SiFs) on glass substrates. SiFs were prepared according to the procedure published previously.¹⁴

Preparation of the MAMEF assay platform for ultra-fast detection of *B. anthracis* DNA. Firstly, in order to prevent the non-specific binding of target DNA and fluorescent probe on the part of the glass slides not covered by silver nanoparticles, all free glass surface amino groups were blocked with freshly prepared succinic anhydride solution (0.156 M in 1-methyl-2-

pyrrolidone, 20 mM borate buffer pH 8.0) for 15 min at room temperature, followed by rinsing with deionized water. SiFs-deposited glass slides were then coated with self-adhesive silicon isolators containing 5 mm-wide circular wells prior to the assay fabrication and subsequent fluorescence experiments.

500 nM of thiolated anchor probe (Fig. 2b) was incubated overnight at 4 °C on the surface of SiFs-deposited glass slides in Hepes buffer (5 mM Hepes, pH 7.5, with final concentrations of 100 mM KCl, 0.25 mM EDTA, this buffer was used in all the experiments unless otherwise stated) followed by rinsing with water to remove the unbound material. The thiolated anchor probe was covalently linked to SiFs *via* well-established, self-assembled monolayer chemistry.³¹ Further surface modification procedures were employed to minimize the non-specific binding of target DNA and the fluorescent probes on to silver nanoparticles, where the anchor probe-modified silver nanoparticles were treated with a 50 μ M aqueous solution of 2-amino(ethoxy)ethanol (AEE) for 2 h. Unbound material was removed by extensive washing. This step significantly reduces the non-specific binding when compared to the previous DNA hybridization data where silver nanoparticles were not treated with AEE.¹⁶

MAMEF-based *B. anthracis* DNA assays using a microwave cavity. The MAMEF-based DNA capture assay was performed by the incubation of varying concentrations of target DNA (synthetic, genomic or exosporium) mixed with TAMRA-labeled fluorescent probe (Fig. 2b) on the anchor probe immobilized on SiFs, in Hepes buffer for 30 s in a microwave cavity (a 0.7 cu ft, GE Compact Microwave Model: JES735BF, max power 700 W). In order to determine the extent of non-specific binding of target DNA mixed with TAMRA-labeled fluorescent probe, an aliquot of the mixture was incubated on the SiFs surface without the thiolated anchor probe for 30 s in a microwave cavity. Experiments pertaining to the non-virulent strain *B. cereus* were performed the same

way. The power setting of the microwave cavity was set to 2, which corresponded to 140 W over the entire cavity. This power is similar to the previous reports using low-power microwaves for immunolabeling,³² immunostaining,³³ in immunocytochemistry³⁴ and histological microwave processing.^{35,36}

Fluorescence spectroscopy. All fluorescence assay measurements were performed by collecting the emission intensity through a long-pass filter (532 nm) perpendicular to the assay surface, after total-internal reflection evanescent wave excitation, using a 532 nm diode laser and a Fiber Optic Spectrometer (HD2000) from Ocean Optics, Inc.

Results and discussion

Assay design and characteristics

The conversion of silver-deposited glass surfaces into MAMEF assay platforms for the ultra-fast detection of the *Bacillus anthracis* target DNA was achieved by attaching an anchor probe specific to the DNA target after the preparation of silver island films (SIFs) on glass surfaces (Fig. 2a). The anchor probe was designed to recognize a nucleotide sequence within the negative strand of the PA gene²⁶ at a region which encodes an area of the protein essential for its biological activity, including a sulfhydryl group at one end (Fig. 2b). The basic attachment chemistry is similar to that used for surface plasmon resonance gold chips^{37,38} and is based on the interaction of silver and sulfhydryl groups on the anchor probe. In order to increase the efficiency of binding of the anchor to the target DNA, at the sulfhydryl end a six-nucleotide region, with the inherent flexibility and which does not bind to the target anthrax DNA, made of thymidines²⁷ was added. In addition, to increase the sensitivity of the assay by reducing the undesired binding of DNA to the assay platform, additional surface modification procedures were employed. These procedures involved the treatment of the *unsilvered* glass and silver surface by chemicals that resisted non-specific binding of DNA.

Ultra-fast detection of synthetic target DNA

The detection of synthetic target DNA was carried out in a single step. A 30 μ L aliquot of target DNA and a fluorescent probe that recognizes a region of the target DNA different from the anchor probe was pipetted on to the MAMEF assay platform, which was then microwave heated for 30 s. At the end of the 30 s microwave heating, the target DNA, the fluorescent and the anchor probe were hybridized (Fig. 2a), resulting in an orange emission at 585 nm (Fig. 1a) when excited with a green laser line (532 nm).

The intensity of the orange emission at 585 nm is directly related to the concentration of the target DNA. The fluorescent probe was designed to be placed very close to the silvered surface (31 nucleotides away) within the enhancement region (>10 nm) of the silver nanoparticles,³⁹ when hybridized with the target DNA (Fig. 2a). An important feature of the design of the anchor and fluorescent probes is that they are designed to bind to the negative strand of the target sequence

within the PA gene (Fig. 2b), and as a consequence they should also be able to bind mRNA transcribed during gene expression, thus increasing the sensitivity of the assay for bacterial lysates.

It is important to note that the silver nanoparticles serve as (i) a platform for the attachment of the anchor probe, (ii) an enhancer of the fluorescence emission,¹⁷ and (iii) a mediator for the localized delivery of the microwave energy that significantly speeds up the hybridization process due to localized heating.¹⁴ The preferential heating of the silver nanoparticles by microwaves is attributed to localized heating as previously described^{40,41} and only results in a minimal increase in the temperature of the bulk medium.

The MAMEF-based ultra-fast detection of *B. anthracis* DNA was first demonstrated using synthetic target DNA in the nanomolar concentration range. Concentration-dependent fluorescence emission data (Fig. 3a) obtained after only 30 s of microwave heating show an intensity increase as increasing concentrations of target DNA are hybridized on the surface assay platform. The increase in emission intensity is also captured visually (Fig. 3b). Control experiments, where the surface-bound anchor probe is omitted, shows minimal emission intensity (less than that of a normal assay) despite the fact that the concentration of target DNA is increased (Fig. 3c). A plot of the intensity at the peak of orange emission (at 585 nm) for the data obtained in the assay and the control experiment (Fig. 3d) shows that the emission intensity at 585 nm is directly related to the solution target DNA concentration for values from 2 to 500 nM.

There are several key features of the data obtained for synthetic target DNA. First, the applicability of the MAMEF technology to a three-piece DNA detection system (one capture, one detector and the target DNA) without any modifications to the target DNA sample was demonstrated. Second, through control experiments the design of the assay platform was proven to be effective in minimizing the non-specific binding of target DNA to the surface. Third, our data show that target DNA can be detected with a signal-to-noise ratio >3 for concentrations down to 5 nM in less than 30 s.

Ultra-fast detection of *B. anthracis* genomic DNA

Genomic DNA extracted from a vegetative culture of the Sterne strain of *B. anthracis* using standard DNA extraction procedures gave a positive signal using the MAMEF assay in the picogram per microliter concentration range. It is important to note the physical differences between the synthetic and genomic DNA: the synthetic DNA comprised a discrete 47 nucleotide sequence designed to maximize interaction with the probes. In contrast, the genomic DNA is a complex mixture of random length DNA pieces including fragments containing the same 47 nucleotide sequence as the synthetic DNA, but surrounded by flanking DNA which could potentially hinder binding to detection probes. The detection procedure for the genomic target DNA was identical to the procedure employed for the detection of the synthetic target DNA. A small volume of sample containing genomic DNA and the fluorescent probe was pipetted on to the assay platform and microwave heated for 30 s.

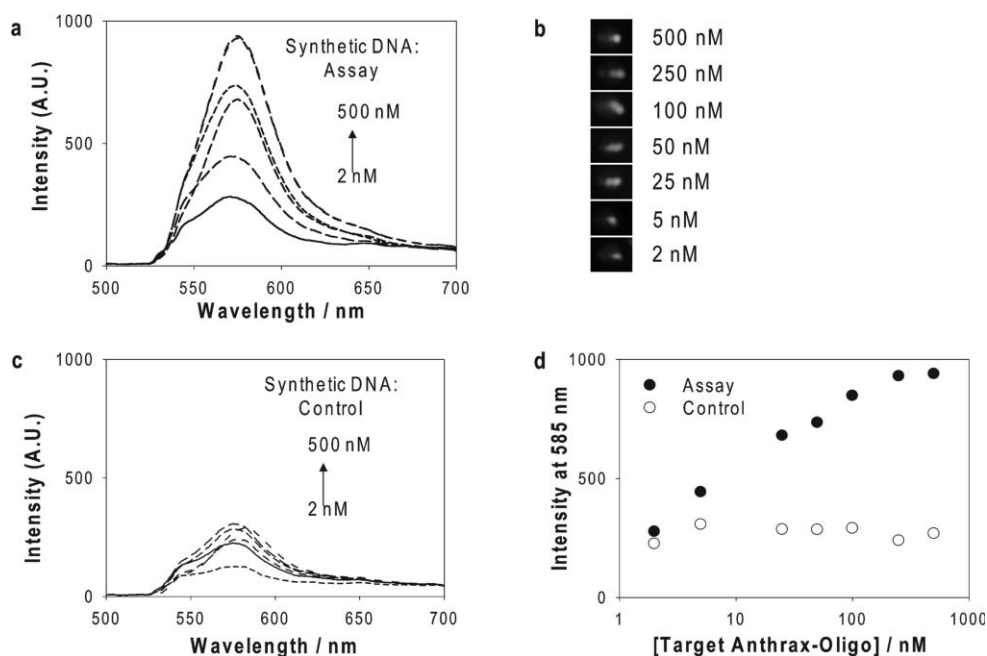


Fig. 3 (a) Emission spectra of TAMRA-oligo as a function of concentration after 30 s of low-power microwave heating. (b) Photographs showing the increased emission intensity visually as a function of TAMRA-DNA concentration after 30 s of low-power Mw heating. (c) A control sample identical to the top-left panel but with no surface-bound anchor probe. (d) Semi-logarithmic plot of the fluorescence emission intensity at 585 nm for the TAMRA-oligo as a function of the target synthetic DNA concentration from the left two panels [(a) and (c)].

Concentration-dependent fluorescence emission data (Fig. 4a) show an increase in emission intensity as the concentration of genomic DNA is increased. Control experiments, where the anchor probe is omitted to determine the extent of non-specific

binding of genomic DNA, show that undesired binding to the assay platform was less than the lowest detection limit of the assay, or $40 \text{ pg } \mu\text{L}^{-1}$ (Fig. 4b). A plot of the emission intensity for the assay and the control experiment shows that the

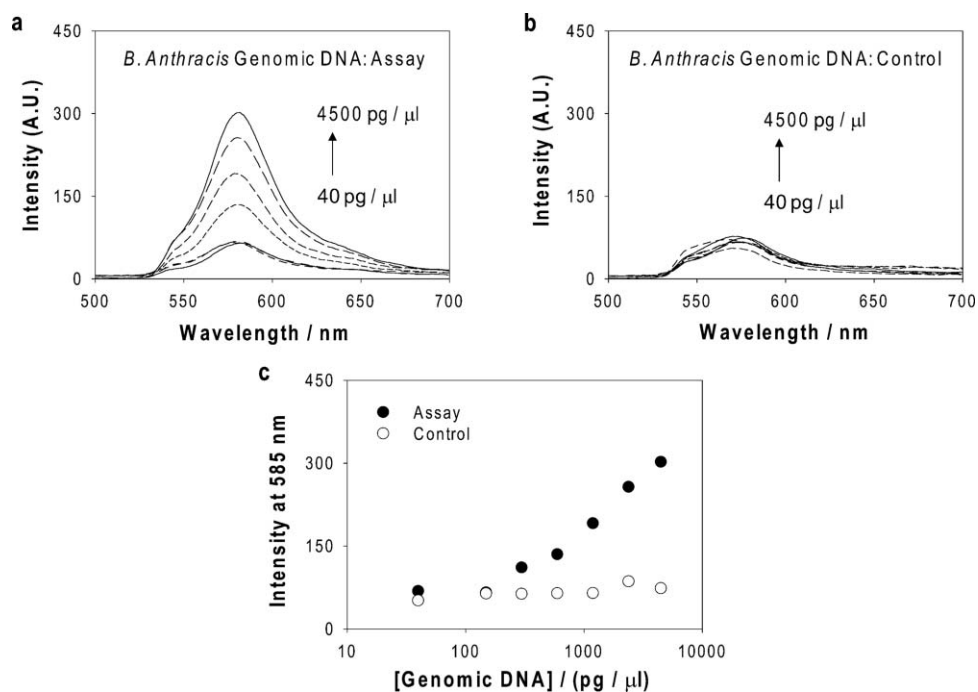


Fig. 4 (a) Emission spectra of TAMRA-oligo as a function of concentration after 30 s of low-power microwave heating with genomic target DNA (*B. anthracis*). (b) A control sample identical to the top-left panel but with no surface-bound anchor probe. (c) Plot of the fluorescence emission intensity at 585 nm for TAMRA-oligo as a function of the target genomic DNA concentration from the top two panels. Sample volume was $30 \text{ } \mu\text{L}$ in all experiments.

emission intensity at 585 nm is directly related to the solution genomic DNA concentration for values from 40 to 4500 pg μL^{-1} (Fig. 4c).

Ultra-fast detection of target DNA on the surface of *B. anthracis* spores

We have also determined the ability of the assay to detect target DNA on the surface of anthrax spores, the form of the organism most likely to be encountered during a biological attack. The spore is constructed inside the vegetative bacterium and is thus covered with cellular debris derived from the mother cell containing cellular proteins, carbohydrates and DNA.⁴² The feasibility of using PCR to detect DNA targets derived from the mother cell on the surface of unprocessed *B. anthracis* spores has been demonstrated with detection times of between 1 and 2 h and a sensitivity limit of 10^2 spores per reaction.^{22,23} We isolated the exosporium, the outer layer of the spore surface formed by members of the *Bacillus cereus* group of organisms which include *B. anthracis*^{29,43} using non-destructive sonication. This loose-fitting, balloon-like layer surrounds the spore and is chemically complex, consisting of structural elements and material adsorbed from the mother cell.²⁹

Aliquots of isolated *B. anthracis* exosporium were mixed with the fluorescent probe (total sample volume was 30 μL) and microwave heated on the MAMEF assay platform for 30 s. Similar to previous results (Fig. 3a; Fig. 4a) an increased concentration of exosporium on the assay resulted in an increased emission intensity (Fig. 5a). The concentration for exosporium DNA was in the nanogram per microliter range. Control experiments, where the anchor probe is omitted to determine the extent of undesired binding of target exosporium DNA, show that undesired binding of target DNA to the assay platform was *significantly* less than the lowest concentration of exosporium DNA detected in the main assay (Fig. 5b). Given that a signal-to-noise (S/N) ratio of 6 [ratio of the emission intensity for the lowest concentration in the assay (Fig. 5a) to the highest emission intensity in the control assay (Fig. 5b)] is obtained here and that a $S/N > 2$ for fluorescence-based assays is considered acceptable,⁴⁴ the actual lower detection limit of the MAMEF-based *B. anthracis* DNA assay is extrapolated to be in the picograms per microliter range. The ability to rapidly detect picogram amounts of target DNA in the presence of the complex organic matrix which comprises the exosporium

strongly suggests that the assay may be equally effective in *unprocessed clinical samples*.

In addition to the rapid detection of low levels of target DNA in the presence of organic material, the assay must be able to distinguish *B. anthracis* from the other members of the genetically closely related *B. cereus* group.⁴⁵ To demonstrate the *specificity* of the assay, exosporium isolated from the *B. cereus* type strain (ATCC 14579) was tested for the presence of target DNA.²⁵ Concentration-dependent fluorescence emission data for the assay (Fig. 6a) and the control sample (Fig. 6b) encouragingly show constant emission intensity for an increased concentration of *B. cereus* exosporium. A plot of all the data for the *B. anthracis* and *B. cereus* exosporium (Fig. 6c) clearly shows the clear distinction of detection range for the anthrax exosporium (assay) from the *B. cereus* (straight line) and for the noise (control).

Finally, to demonstrate the specificity of the assay for a sample that contains a mixture of DNA from both strains at once, a mixture of (same initial concentrations, 50% v/v) exosporium from *B. anthracis* and *B. cereus* was tested for successful detection of target DNA. Concentration-dependent fluorescence emission data for the assay (Fig. 7a) show a significant increase in fluorescence emission with the concentration of exosporium (and fluorescent probe) whereas only a slight increase in intensity for the control assay (Fig. 7b). A plot of concentration-dependent emission intensity at 585 nm shows the range of detection for *B. anthracis* DNA in a mixture of exosporium DNA from two *Bacillus* strains. It is important to note that the slight increase in the control assay (Fig. 7b) is due to non-specific binding of exosporium DNA as seen in Fig. 5b and Fig. 6b.

Discussion

In this paper, we have demonstrated the ultra-fast detection of *Bacillus anthracis* specific target DNA using a relatively simple and inexpensive assay platform technology, microwave-accelerated metal-enhanced fluorescence (MAMEF). MAMEF technology, a combination of the metal-enhanced fluorescence technology that increases the sensitivity of fluorescence-based assays and microwave heating to kinetically accelerate the biomolecular recognition events, afforded the one-step detection of target DNA on the surface of *B. anthracis* spores after only 30 s of very low-power microwave heating.

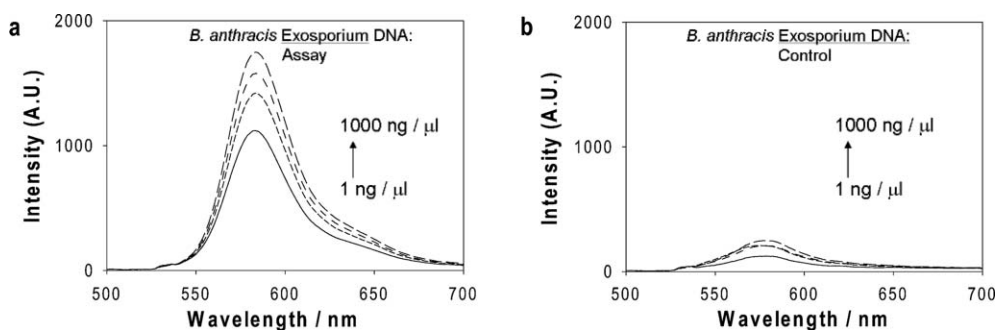


Fig. 5 (a) Emission spectra of TAMRA-oligo as a function of *B. anthracis* exosporium concentration after 30 s of low-power microwave heating. (b) A control sample identical to the left panel but with no surface-bound anchor probe. Sample volume was 30 μL in all experiments.

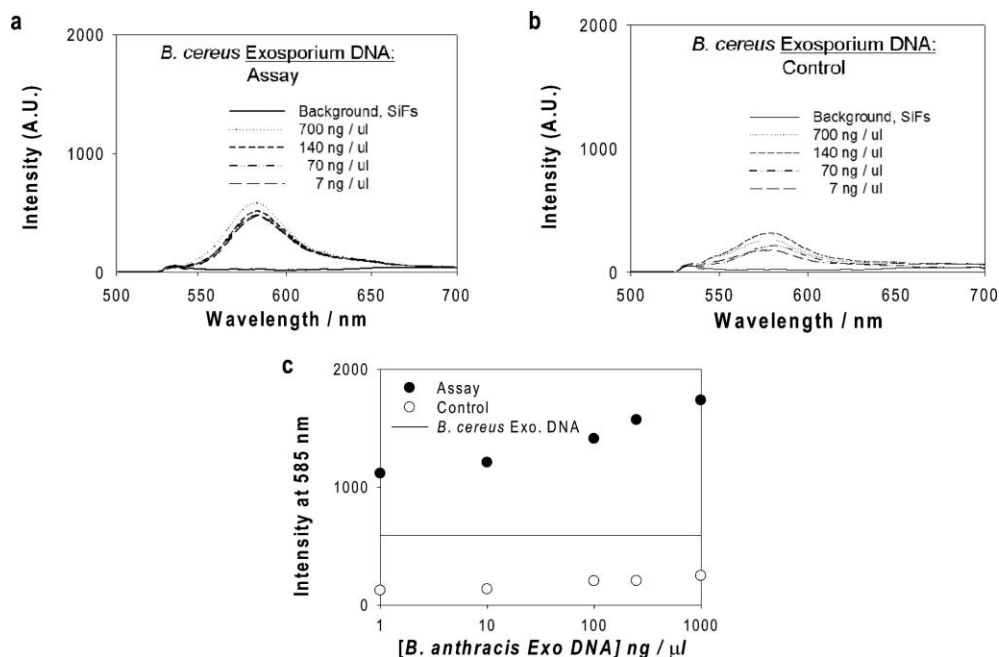


Fig. 6 (a) Emission spectra of TAMRA-oligo as a function of *B. cereus* exosporium concentration after 30 s of low-power microwave heating. (b) A control sample identical to the top-left panel but with no surface-bound anchor probe. Background fluorescence from SiFs (no TAMRA-oligo) is also shown. (c) Semi-logarithmic plot of the fluorescence emission intensity at 585 nm for TAMRA-oligo as a function of *B. anthracis* exosporium concentration obtained from Fig. 5. The horizontal line shows the emission intensity at 585 nm obtained from assays using *B. cereus* (Fig. 6a). Sample volume was 30 μ L in all experiments.

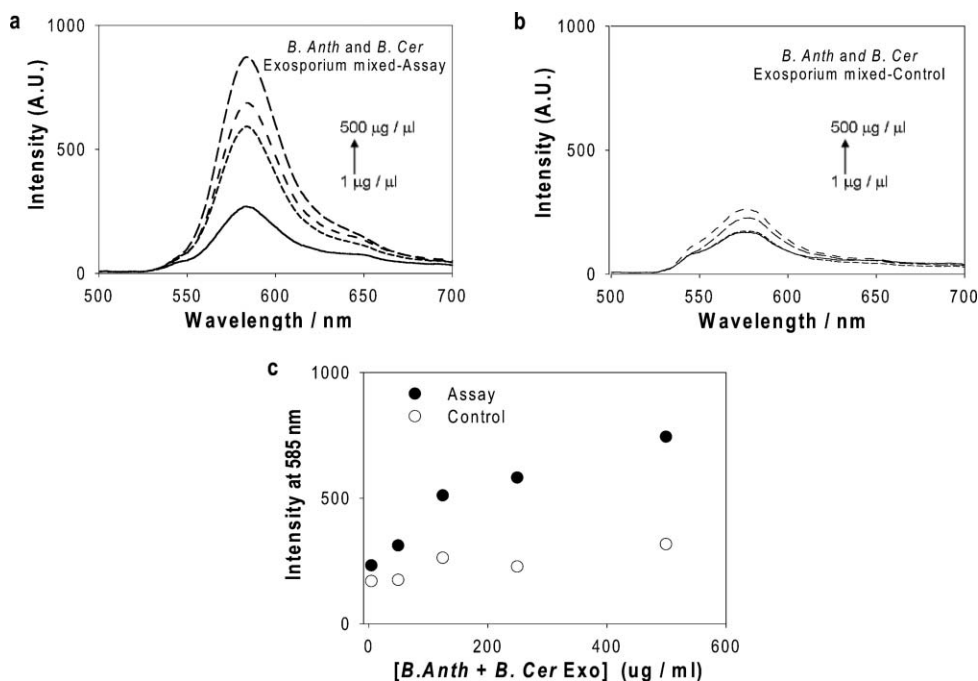


Fig. 7 (a) Emission spectra of TAMRA-oligo as a function of a mixture of *B. cereus* and *B. anthracis* exosporium concentration after 30 s of low-power microwave heating. (b) A control sample identical to the top-left panel but with no surface-bound SH-oligo (anchor probe). (c) Plot of the fluorescence emission intensity at 585 nm for TAMRA-oligo as a function of target concentration.

The design of the silver nanoparticle-deposited MAMEF assay platforms makes several key features of the MAMEF technology possible, including the enhancement of fluorescence emission by localized silver colloids and the localized

heating for faster hybridization kinetics. The temperature change of the solution above the SiFs, due to microwave heating, was previously determined by our group using temperature-dependent fluorescent probes.¹⁶ For a 30 s

DNA hybridization assay, it is estimated that the temperature of the bulk medium above the SiFs increased from 23 to 28 °C.¹⁶ The increase in the temperature around the silver nanoparticles is believed to be higher due to localized heating around/on the nanoparticles, which results in faster hybridization kinetics. It was also found that 30 s of low-power microwave heating of DNA in close proximity to silver nanoparticles *did not* cause denaturation of DNA strands.⁴⁶ This was demonstrated using a simple series of experiments: first, a double-stranded DNA tagged with a fluorophore on silver nanoparticles was dehybridized by conventional heating of DNA beyond its melting point and washing of the solution and, second, microwave heating a new aliquot of the same complementary strand on silver nanoparticles resulted in a return of the almost identical fluorescence emission intensities.⁴⁶ This is attributed to the preferential heating of the silver nanoparticles and localized dissipation of heat to their immediate environment resulting in faster hybridization kinetics but without causing denaturation of DNA.

In addition to the benefits of using silver nanoparticles mentioned above, silver nanoparticles also provided the means of attaching the anchor probes to the assay platform through thiol surface chemistry. That is, the anchor probes are only present on the silver nanoparticles but not on glass, and subsequent hybridization of DNA only occurs on the silver nanoparticles, which is crucial for the enhancement of fluorescence and the localized delivery of heat by the silver nanoparticles. Additional surface modifications to glass and silver nanoparticles were employed to minimize the undesired binding of non-specific DNA, which could potentially lead to false positives.

Another interesting feature of the design of the MAMEF-based detection assay for *B. anthracis* target DNA is that the anchor and fluorescent probes are designed in such a way that they bind to the negative strand of the target DNA-specific sequence (Fig. 2b), but these probes are also able to bind mRNA transcribed from this strand, potentially increasing the sensitivity/detectability of the assay.

Finally, the genomic DNA and exosporium DNA used in this study were obtained following a number of pre-processing steps. It might be possible to minimize these steps by employing much higher power and highly focused microwaves, which are likely to disrupt the *B. anthracis* spores, and potentially allow the recovery of the relevant anthrax DNA. When this approach is incorporated into the MAMEF detection scheme, the overall two-step anthrax detection could then be completed in less than a few minutes, a significant benefit as compared to current technologies which take >2 h.

Conclusions

In conclusion, this study illustrates the two levels of scientific research conducted for the development of an ultra-fast anthrax detection system that will affect human life in the case of an anthrax attack: the *proof-of-principle* demonstration of a technology and *translation of the technology* into a solution for a real life problem. Firstly, the *proof-of-principle* of the MAMEF technology for the ultra-fast detection of synthetic *Bacillus anthracis* target DNA was demonstrated.

The synthetic DNA has a defined length of nucleotides and purified to remove irrelevant biomolecules. MAMEF-based detection of 'laboratory'-derived *B. anthracis* target DNA showed a sensitivity of nanomolar concentrations detected *within only a few seconds*. Secondly, the translation of the MAMEF technology to ultra-fast and sensitive detection of target DNA against a background of genomic DNA was successfully accomplished. Genomic target DNA present in the exosporium of *B. anthracis* spores was detected within a minute in the nanograms per microliter concentration range using an assay platform with carefully designed components and simple, low cost, low-power microwave heating. The MAMEF technology was able to clearly distinguish between *B. anthracis* and *B. cereus*, a non-virulent close relative. We believe that this study has set the stage and path for the ultra-fast and specific detection of *B. anthracis* spores with minimal pre-processing steps using a relatively simple but effective technology that could minimize casualties in the event of another anthrax attack.

Acknowledgements

This work was supported by the Middle Atlantic Regional Center of Excellence for Biodefense and Emerging Infectious Diseases Research (NIH NIAID - U54 AI057168). Salary support to authors from UMBI and the IoF are also acknowledged.

References

- 1 C. L. Selinsky, V. D. Whitlow, L. R. Smith, D. C. Kaslow and H. M. Horton, *Biologicals*, 2007, **35**, 123–129.
- 2 D. Rodriguez-Lazaro, M. Hernandez, M. D'Agostino and N. Cook, *J. Rapid Methods Automat. Microbiol.*, 2006, **14**, 218–236.
- 3 T. C. Dixon, M. Meselson, J. Guillemin and P. C. Hanna, *New Engl. J. Med.*, 1999, **341**, 815–826.
- 4 D. R. Franz, P. B. Jahrling, A. M. Friedlander, D. J. McClain, D. L. Hoover, W. R. Bryne, J. A. Pavlin, C. W. Christopher and E. M. Eitzen, *J. Am. Med. Assoc.*, 1997, **278**, 399–411.
- 5 H. Smith and J. Keppie, *Nature*, 1954, **173**, 869–870.
- 6 H. Smith, J. Keppie, J. L. Stanley and H.-S. PW, *Br. J. Exp. Pathol.*, 1955, **36**, 323–335.
- 7 L. Baillie and T. D. Read, *Curr. Opin. Microbiol.*, 2001, **4**, 78–81.
- 8 X. Y. Zhang, N. C. Shah and R. P. Van Duyne, *Vib. Spectrosc.*, 2006, **42**, 2–8.
- 9 X. Y. Zhang, M. A. Young, O. Lyandres and R. P. Van Duyne, *J. Am. Chem. Soc.*, 2005, **127**, 4484–4489.
- 10 R. E. Biagini, D. L. Sammons, J. P. Smith, B. A. MacKenzie, C. A. Striley, J. E. Snawder, S. A. Robertson and C. P. Quinn, *Clin. Vaccine Immunol.*, 2006, **13**, 541–546.
- 11 C. Guarise, L. Pasquato, V. De Filippis and P. Scrimin, *Proc. Natl. Acad. Sci. U. S. A.*, 2006, **103**, 3978–3982.
- 12 M. E. Cullum, L. A. Lininger, S. Z. Schade, S. E. Cope, J. C. Ragain, Jr. and L. G. Simonson, *Military Med.*, 2003, **168**, 915–921.
- 13 R. T. Cummings, S. P. Salowe, B. R. Cunningham, J. Wiltsie, Y. W. Park, L. M. Sonatore, D. Wisniewski, C. M. Douglas, J. D. Hermes and E. M. Scolnick, *Proc. Natl. Acad. Sci. U. S. A.*, 2002, **99**, 6603–6606.
- 14 K. Aslan and C. D. Geddes, *Anal. Chem.*, 2005, **77**, 8057–8067.
- 15 K. Aslan, P. Holley and C. D. Geddes, *J. Immunol. Methods*, 2006, **312**, 137–147.
- 16 K. Aslan, S. N. Malyn and C. D. Geddes, *Biochem. Biophys. Res. Commun.*, 2006, **348**, 612–617.
- 17 K. Aslan, I. Gryczynski, J. Malicka, E. Matveeva, J. R. Lakowicz and C. D. Geddes, *Curr. Opin. Biotechnol.*, 2005, **16**, 55–62.

-
- 18 K. Aslan, J. Huang, G. M. Wilson and C. D. Geddes, *J. Am. Chem. Soc.*, 2006, **128**, 4206–4207.
- 19 K. Aslan, Z. Leonenko, J. R. Lakowicz and C. D. Geddes, *J. Phys. Chem. B*, 2005, **109**, 3157–3162.
- 20 K. Aslan, Z. Leonenko, J. R. Lakowicz and C. D. Geddes, *J. Fluoresc.*, 2005, **15**, 643–654.
- 21 K. Aslan, M. J. R. Previte, Y. X. Zhang and C. D. Geddes, *Biophys. J.*, 2007, 371A–371A.
- 22 T. C. Reif, M. Johns, S. D. Pillai and M. Carl, *Appl. Environ. Microbiol.*, 1994, **60**, 1622–1625.
- 23 H. Ellerbrok, H. Nattermann, M. Ozel, L. Beutin, B. Appel and G. Pauli, *FEMS Microbiol. Lett.*, 2002, **214**, 51–59.
- 24 M. A. Weiner, T. D. Read and P. C. Hanna, *J. Bacteriol.*, 2003, **185**, 1462–1464.
- 25 N. Ivanova, A. Sorokin, I. Anderson, N. Galleron, B. Candelon, V. Kapatral, A. Bhattacharyya, G. Reznik, N. Mikhailova, A. Lapidus, L. Chu, M. Mazur, E. Goltsman, N. Larsen, M. D'Souza, T. Walunas, Y. Grechkin, G. Pusch, R. Haselkorn, M. Fonstein, S. D. Ehrlich, R. Overbeek and N. Kyrpidis, *Nature*, 2003, **423**, 87–91.
- 26 S. L. Welkos, J. R. Lowe, F. Edenmccutchan, M. Vodkin, S. H. Leppla and J. J. Schmidt, *Gene*, 1988, **69**, 287–300.
- 27 S. D. Goodman and O. Kay, *J. Biol. Chem.*, 1999, **274**, 37004–37011.
- 28 L. Baillie, S. Hibbs, P. Tsai, G. L. Cao and G. M. Rosen, *FEMS Microbiol. Lett.*, 2005, **245**, 33–38.
- 29 C. Redmond, L. W. J. Baillie, S. Hibbs, A. J. G. Moir and A. Moir, *Microbiology*, 2004, **150**, 355–363.
- 30 T. J. Kang, M. J. Fenton, M. A. Weiner, S. Hibbs, S. Basu, L. Baillie and A. S. Cross, *Infect. Immun.*, 2005, **73**, 7495–7501.
- 31 K. Aslan and V. H. Perez-Luna, *Langmuir*, 2002, **18**, 6059–6065.
- 32 L. Chicoine and P. Webster, *Microsc. Res. Tech.*, 1998, **42**, 24–32.
- 33 K. D. Micheva, R. W. Holz and S. J. Smith, *J. Cell Biol.*, 2001, **154**, 355–368.
- 34 L. K. Rangell and G. A. Keller, *J. Histochem. Cytochem.*, 2000, **48**, 1153–1159.
- 35 D. Schichnes, J. Nemson, L. Sohlberg and S. E. Ruzin, *Microsc. Microanal.*, 1998, **4**, 491–496.
- 36 U. A. Rassner, D. A. Crumrine, P. Nau and P. M. Elias, *Histochem. J.*, 1997, **29**, 387–392.
- 37 B. Liedberg, I. Lundstrom and E. Stenberg, *Sens. Actuators, B*, 1993, **11**, 63–72.
- 38 B. Liedberg, C. Nylander and I. Lundstrom, *Biosens. Bioelectron.*, 1995, **10**, R1–R9.
- 39 J. R. Lakowicz, *Anal. Biochem.*, 2001, **298**, 1–24.
- 40 K. Hamad-Schifferli, J. J. Schwartz, A. T. Santos, S. G. Zhang and J. M. Jacobson, *Nature*, 2002, **415**, 152–155.
- 41 M. J. Kogan, N. G. Bastus, R. Amigo, D. Grillo-Bosch, E. Araya, A. Turiel, A. Labarta, E. Giralt and V. F. Puntes, *Nano Lett.*, 2006, **6**, 110–115.
- 42 J. L. Almeida, L. L. Wang, J. B. Morrow and K. D. Cole, *J. Res. Natl. Inst. Standards Technol.*, 2006, **111**, 205–217.
- 43 S. Charlton, A. J. Moir, L. Baillie and A. Moir, *J. Appl. Microbiol.*, 1999, **87**, 241–245.
- 44 J. R. Lakowicz, *Principles of Fluorescence Spectroscopy*, Kluwer Academic, New York, 2nd edn, 1999.
- 45 L. W. Baillie, *Letts. Appl. Microbiol.*, 2005, **41**, 227–229.
- 46 K. Aslan, S. N. Malyn, G. Bector and C. D. Geddes, *Analyst*, 2007, DOI: 10.1039/b708069g.